

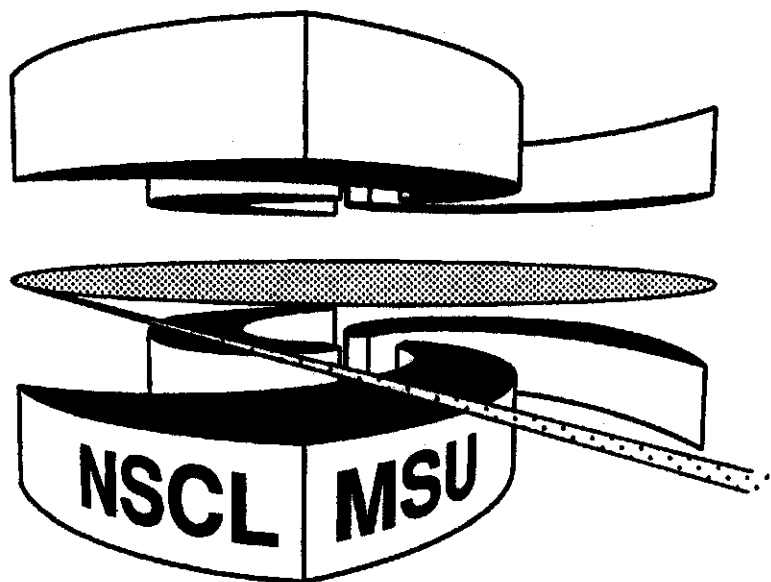


Michigan State University

National Superconducting Cyclotron Laboratory

**ASPECTS OF THE STRUCTURE OF LIGHT NUCLEI**

**B. ALEX BROWN**



MSUCL-941

AUGUST 1994

# ASPECTS OF THE STRUCTURE OF LIGHT NUCLEI \*

B. ALEX BROWN

*Department Of Physics and Astronomy,  
and National Superconducting Cyclotron Laboratory,  
Michigan State University, E. Lansing, MI 48824, USA*

## ABSTRACT

There are many interesting aspects to the structure of light nuclei ( $A < 40$ ). In this paper I organize these in terms of 30 individual but interrelated topics.

### 1. Simple Shell-Model Structure

The nuclear shell model is an excellent starting point for understanding the observed properties of light nuclei.  $^{16}\text{O}$  and  $^{40}\text{Ca}$  provide the well-known doubly-closed shell nuclei, and the observed properties of the neighboring odd-even nuclei are qualitatively as one expects for single-particle states. The shell-model provides a basis upon which more complete and complicated wave functions can be built. The division into the major-oscillator shells, Os, Op, Ods and Ofp, provides a particularly good zeroth-order basis.

Many levels in nuclei with  $N=2-8$  and  $Z=2-8$  are understood (in zeroth order) in terms of Op shell configurations, and many levels in nuclei with  $N=8-20$  and  $Z=8-20$  are understood in terms of Ods shell configurations. <sup>1</sup> Cross shell Op-Ods configurations are represented by the low-lying levels in nuclei with  $N=8-20$  and  $Z=2-8$ , as well as by excited states in other nuclei, such as the well-known 4p-4h state in  $^{16}\text{O}$ . There are also cases where the structures in terms of major-oscillator configuration are strongly mixed (in the case of nearly degenerate simple configurations) or are more complicated (as in the case of loosely bound di-nucleons, some alpha-cluster configurations, or very deformed configurations.)

### 2. $N\hbar\omega$ Excitations and Spurious States

It is well known that the shell-model configurations are a mixture of intrinsic excitations and center-of-mass (spurious) excitations. The lowest  $0\hbar\omega$  configurations are particularly simple, since the center of mass is in a Os state. <sup>2</sup> In order to completely separate out the spurious states, the basis must be constructed in a full  $N\hbar\omega$  configuration space. For example, the  $[0p_{1/2}^{-1}1s_{1/2}](J^{\pi}=1^{-}, T=0)$  configuration is partly intrinsic and partly spurious. To remove the spurious state component, the full  $0p^{-1}$ -Ods configuration space must be used. A particularly simple method for removing the spurious component is to add a fictitious Hamiltonian which acts only upon the

---

\*Invited paper presented at the International Symposium on Frontiers of Nuclear Structure Physics, Interactions in Hadrons and Nuclei, RIKEN, Japan, March 2-5, 1994

center-of-mass and whose function is to push up the spurious states to a high excitation energy.<sup>3</sup> In practical applications, however, there are several important questions to be addressed. One might want to carry out a 0p-0d1s calculation which would include many excitations across these two major shells. For example, the 4p-4h excited states in  $^{16}\text{O}$  are, in general, partly spurious, and one must use a  $4\hbar\omega$  basis. The full 0p-0d1s basis would include parts of up to  $12\hbar\omega$  excitations, and in order to remove the spurious states, one must include 14 major-oscillator shells – a calculation which is clearly not tractable. However, perhaps to some good approximation, some of the physical states of interest are made up of classes of states (e.g. which one can find in the SU3 basis) which only require the 0p-0d1s basis. Further investigation is needed.

### 3. The Hartree-Fock Condition

When the shell-model basis is truncated to the lowest  $0\hbar\omega$  configuration, there is a simple relationship between  $\hbar\omega$  and the nuclear rms radius which can be used to obtain a value for  $\hbar\omega$ . When the basis is expanded to include both  $0\hbar\omega$  and  $2\hbar\omega$ , 1p-1h ( $2\hbar\omega$ ) states become mixed into the 0p-0h ( $0\hbar\omega$ ) states. In this case, the relationship between  $\hbar\omega$  and the nuclear rms radius is more complicated and is interaction dependent. One may try to adjust  $\hbar\omega$  in the  $(0+2)\hbar\omega$  space in order to minimize the energy; however, this may not give the correct rms radius. It is well known that the effective interactions used in Hartree-Fock calculations which give both the correct binding energy and rms radius (i.e. interactions which have the correct saturation property) are phenomenologically rather complicated – they have a strong density dependence which makes the interaction weaker in the nuclear interior. Interactions used in shell-model calculations may not be compatible with this property. Various methods have been introduced in order to enforce the “Hartree-Fock condition” even when the shell-model interactions themselves do not have the correct saturation property.<sup>4,5,6</sup> This point, however, needs further investigation. Ideally one should use an interaction for the shell-model calculation which has the correct saturation properties.

### 4. Effective Interactions in the 0p and 0d1s Model Space

It is well known that phenomenological interactions can be obtained for the 0p and 0d1s model spaces which semi-quantitatively describe the experimental data.<sup>1</sup> It is possible to derive nearly model-independent interactions for these regions by carrying out a fit of the single-particle energies and two-body interaction matrix elements to the large body of experimental data. The obtained interaction is model-independent in the sense that the single-particle energies and most of the two-body matrix elements are well determined by the energy-level data, and that by fitting the two-body matrix elements one does not have to make an assumption about the structure of the effective interaction. The basic assumption behind this approach is that the two-body matrix elements themselves are the same for every energy level and every nucleus, with, at most, a smooth mass dependence. The phenomenological effective interactions

turn out to be close in appearance to the Kuo-Brown G matrix elements, but their differences are important on the quantitative level.<sup>7</sup> It is important, but probably very difficult, to try to understand the origin of the differences. I also note that the experimental energy-level data can be almost equally well reproduced by starting with a one-boson-exchange OBEP model for the interaction which has relatively few parameters.<sup>7</sup>

## 5. Cross-Shell 0p-0d1s Effective Interactions for Pure $N\hbar\omega$ Configurations

The model-independent (two-body matrix element) method is not so reliable for the cross-shell because the the number of two-body matrix elements is comparable to the number of experimental data. Alternatively, one may try to adjust the parameters of a OBEP model to fit the cross-shell data. Millener and Kurath<sup>8</sup> originally used the OBEP method. The 0p-0d1s cross-shell interaction has more recently been investigated in terms of both the model-independent and OBEP methods. The interactions derived from a fit to 165 cross-shell energy-level data are denoted by WBT and WBP, respectively.<sup>9</sup> The rms deviation between the calculated and experimental energy level data in the mass region  $A=10-22$  was about 330 keV. With the OBEP method, harmonic-oscillator radial wave functions were used to calculate the two-body matrix elements. In both cases the states are assumed to be described by pure  $N\hbar\omega$  configurations, and only those data where the level is known to be rather pure were considered.

When the WBT or WBP interactions are used to calculate the energies of the pure  $0^+$ ,  $T=0$  configurations in  $^{16}\text{O}$ , the excitation energies of the  $2\hbar\omega$  and  $4\hbar\omega$  configurations come out at about 9 MeV and 6 MeV, respectively, in reasonable agreement with where these states are experimentally observed in cluster transfer reactions. This is also the case for other nuclei in this mass region. This agreement is perhaps surprising, but can be understood in terms of the weak-coupling models developed many years ago by Arima et al.<sup>10</sup> and others.<sup>11</sup>

## 6. Mixed Cross-Shell 0p-0d1s Configurations

It is important to study the mixing of  $N\hbar\omega$  configurations. As a prototype, we can consider the mixing of the 0, 2 and  $4\hbar\omega$  configurations for  $^{16}\text{O}$ . When our WBT interaction<sup>9</sup> is used, the mixing between the  $N\hbar\omega$  configurations is very large.<sup>4</sup> The state which is predominantly  $2\hbar\omega$  comes out at about the right excitation energy, however, the state which is predominantly  $4\hbar\omega$  comes out about 11 MeV to high compared to the well-known state at 6 MeV. This is understood from the fact that the mixed ground state is pushed down by about 11 MeV relative to the pure  $0\hbar\omega$  energy by the admixture of the 2 and 4  $\hbar\omega$  configurations. However, the comparable 6 and 8  $\hbar\omega$  configurations which are needed to push down predominantly  $4\hbar\omega$  states are not present in the model space. It is the  $SU_3(20)$  component of the off-diagonal  $\Delta\hbar\omega=2\hbar\omega$  interaction which is responsible for this shift. We have proposed<sup>4</sup> a simple "shift" method to take into account this truncation. This shift can also be regarded

in some approximation as giving rise to an effective gap reduction between the  $0p$  and  $0d_{1s}$  shells as used by Haxton and Johnson.<sup>12</sup>

## 7. Cross-Shell Effective Interactions for Mixed $N\hbar\omega$ Configurations

Another problem in the mixed  $N\hbar\omega$  model space is the effective interaction. It is really not appropriate to use our WBT or WBP interactions in the mixed space because they were derived from wave functions in the pure  $N\hbar\omega$  model space. Its use in the mixed space results in some double counting. Others have used the bare  $G$  matrix in the mixed space.<sup>12</sup> An effective interaction has been obtained from a fit to data in an  $(0+2)\hbar\omega$  model space,<sup>13</sup> however, inconsistencies in the methodology have been pointed out.<sup>14</sup> New work has also begun on the  $G$  matrix for mixed  $N\hbar\omega$  configurations in light nuclei.<sup>15</sup> The derivation of a good effective interaction for the mixed  $N\hbar\omega$  model space in light nuclei will be an important future project.

## 8. Parity Inversion in $^{11}\text{Be}$

The ground state  $J^\pi = 1/2^+$  for  $^{11}\text{Be}$  is one of the outstanding exceptions to the simplest shell-model picture. New  $1\hbar\omega$  calculations<sup>9,16</sup> provide an opportunity for a quantitative understanding of this feature which has long been of theoretical interest.<sup>17</sup> One can account for the energy gap between the  $1/2^+$  ground state and  $1/2^-$  excited state at 0.32 MeV in terms of three distinct physical contributions. First (i), the  $1s_{1/2}$  single-particle energy is calculated to lie about 3.6 MeV higher than the  $0p_{1/2}$  single-particle energy within the the  $0\hbar\omega$  spherical mean-field (monopole) part of our WBT interaction in  $^{12}\text{Be}$ . However, there are two configuration mixing (correlation) effects which lower the energy of the  $1/2^+$  configuration in  $^{11}\text{Be}$ . (ii) There is an extra pairing energy in the  $1/2^+$  configuration due to the two neutron holes in the  $0p$  shell, which lowers the  $1/2^+$  configuration (relative to the  $1/2^-$  configuration) by about 2.2 MeV. Also, (iii) there is mixing with the  $[2^+ \otimes d_{5/2}](1/2^+)$  configuration via the deforming  $Q:Q$  interaction, which lowers the energy by about 1.5 MeV. Adding up (i), (ii) and (iii), the  $1/2^+$  and  $1/2^-$  configurations become essentially degenerate. This degeneracy appears to be due to an accidental cancellation of several effects and not fundamental – but this aspect would be interesting to explore further.

## 9. Parity Inversion in $^{10}\text{Li}$

The interplay of the three mechanisms discussed above for the parity-inversion in  $^{11}\text{Be}$  are responsible for similar phenomena in other nuclei. In particular, recent investigations of resonances in  $^{10}\text{Li}$  have suggested the presence of a narrow low-lying  $s$ -wave.<sup>18</sup> Barker and Hickey have suggested that there may be a parity inversion in  $^{10}\text{Li}$ , and our WBT and WBP interactions also predict a parity inversion in  $^{10}\text{Li}$ . In detail, the calculated  $(0+1)\hbar\omega$  spectrum of  $^{10}\text{Li}$  with the WBT interaction is  $2^-(\text{gs})$ ,  $1^+(0.10 \text{ MeV})$ ,  $2^+(0.32 \text{ MeV})$ ,  $1^-(1.30 \text{ MeV})$ ,  $0^-(1.93 \text{ MeV})$  and eleven more levels up to 4 MeV. Experimental confirmation is important not only from the point of

view of the unusual narrowness of s-wave resonances near threshold, but also for the structure of  $^{11}\text{Li}$ .

## 10. Intruder States in $^{12}\text{Be}$ , $^{11}\text{Li}$ and $^{10}\text{He}$

Parity inversion is closely related to the problem of intruder states. When the WBT interaction is applied to the pure  $N\hbar\omega$  configurations of the  $N=8$  isotones, the pure  $1\hbar\omega$  excitations always lie several MeV above the ground state – there is no parity inversion. However, it is remarkable to find that the  $2\hbar\omega$  excitations which start out at 9 MeV in  $^{16}\text{O}$  quickly come down in energy (8 MeV in  $^{15}\text{N}$ , 5 MeV in  $^{14}\text{C}$  and 3 MeV in  $^{13}\text{B}$ ) until they become essentially degenerate with the  $0\hbar\omega$  configuration in  $^{12}\text{Be}$ ,  $^{11}\text{Li}$  and  $^{10}\text{He}$ . When the  $0\hbar\omega$  and  $2\hbar\omega$  configurations are allowed to mix in these three nuclei, there will be two states each with about 50-50 admixtures of  $0\hbar\omega$  and  $2\hbar\omega$ . There are, in contrast, shell-model calculations for  $^{11}\text{Li}$  in which the  $2\hbar\omega$  component is small<sup>19</sup> or absent,<sup>20</sup> due to the fact that the “shift” problem described above was not taken into account or the  $0d_{1/2}$  shell was ignored.

## 11. Intruder States in the Region $^{32}\text{Mg}$

The same mechanisms which produce the parity inversion and intruder states in the  $^{11}\text{Li}$  region are important for all nuclei. But they are especially important for the region of  $^{32}\text{Mg}$  where the  $2\hbar\omega$  intruder states energies lie several MeV below the  $0\hbar\omega$  energies, giving rise to an “island of inversion.” The calculations are well documented in the literature<sup>21,22,23</sup> – perhaps theory is slightly ahead of experiment in this region. New experiments with radioactive beams will be interesting to explore.

## 12. Properties of $^{11}\text{Li}$

The drip-line nucleus  $^{11}\text{Li}$  is not only very loosely bound to two-neutron decay; it also lies in a complex shell-model region. This complexity is partly related to the coupling to excited states in  $^9\text{Li}$ . Although it is very appropriate to discuss  $^{11}\text{Li}$  in a three-body model, up to now the calculations take into account the coupling with the ground state of  $^9\text{Li}$ . The single-particle energy gap between the  $1s_{1/2}$  and  $0p_{1/2}$  states is about 3 MeV in  $^{11}\text{Li}$ , but the pairing energy and the coupling to the  $^9\text{Li}$  excited states will make these two states effectively degenerate.

It would also be interesting to look for drip-line nuclei which are loosely bound to two-neutron decay, but whose shell-model structure is simpler – such as the neutron-rich C isotopes.  $^{26}\text{O}$  is an interesting case where the  $0d_{1/2}$  shell calculations predict a very small (but not clearly bound or unbound?) two-neutron separation energy.<sup>24</sup>

## 13. Properties of $^{12}\text{Be}$

Barker<sup>25</sup> has pointed out the possibility for a mixed  $(0+2)\hbar\omega$  configuration for the  $^{12}\text{Be}$  ground state. One of the most direct radioactive beam experiments which would

test the structure of the  $^{12}\text{Be}$  ground state is the pick-up of one neutron leading to the parity doublet in  $^{11}\text{Be}$  (with a resolution capable of separating the 0.32 MeV doublet). A pure  $0\hbar\omega$  configuration would lead only to the  $1/2^-$  final state, whereas the mixed configuration will also lead to the  $1/2^+$  final state (the calculated spectroscopic factor is about 0.4). A better experimental and theoretical understanding of the excited states of  $^{12}\text{Be}$  is needed.

#### 14. Neutron Halos

Larger than normal matter rms radii first showed up experimentally in terms of the enhanced reaction cross sections for scattering of radioactive beams off of light and heavy target nuclei.<sup>26</sup> This has been interpreted in terms of loosely bound valence neutrons. Hartree-Fock calculations in which the valence neutrons are constrained to match the experimental separation energies can qualitatively explain the cross section data.<sup>27</sup> The valence neutron density from such calculations has a long tail whose fall-off is governed by the neutron separation energies.<sup>28,29</sup> One perhaps thinks of a halo in the case where most of the valence matter (neutron) density lies outside that of the core density. Although for the nuclei investigated thus far, this is probably not the case; nevertheless there is a significant fraction of the valence density at a large radius (and the valence rms radius is large), and they are referred to as neutron halos. (Of course, the distinction between valence and core neutron densities is a theoretical concept, but one can experimentally distinguish the proton and neutron distributions.)

The above qualitative picture should be semi-quantitative in the cases where the nucleus is loosely bound to one-neutron decay but more strongly bound to two-neutron decay, because the Hartree-Fock (single-particle mean field) picture more applicable. For example, the  $B(E1)$  for the  $1/2^-$  to  $1/2^+$  transition in  $^{11}\text{Be}$ , calculated in a Woods-Saxon model in which the valence orbitals are constrained to their experimental separation energies, is large and agrees with the experimental  $B(E1)$ .<sup>30</sup> To some extent the extreme shell model picture becomes better for loosely bound states because valence-core interaction (which is responsible for retarding low-lying  $E1$  transitions and enhancing low-lying  $E2$  transitions) becomes weaker.

When the nucleus is loosely bound to two-neutron decay, the situation is much more complicated in the traditional shell-model language, and a three-body model is more appropriate. The phenomena in heavier nuclei, where there are a large number of fairly loosely bound valence neutrons, has been referred to as a neutron "skin," and the traditional Hartree-Fock method should again be applicable.<sup>31</sup>

#### 15. Proton Halos

The Coulomb barrier prevents loosely bound protons from extending as far as the loosely bound neutrons. The most extreme case to consider is that for a loosely bound  $1s_{1/2}$  state, since the centrifugal barrier is small. The  $1/2^+$  first excited state of  $^{17}\text{F}$  which is bound by only 100 keV provides a good example. The valence radius

of this state is calculated<sup>32</sup> to be 5.5 fm – twice as large as the rms radius of the  $^{16}\text{O}$  core (2.7 fm). But, unfortunately, this excited state cannot be studied directly. The  $B(E2)$  for the transition to the  $^{17}\text{F}$  ground state ( $1s_{1/2} \rightarrow 0d_{5/2}$ ) is much larger than any other “single-particle” transition in this mass region.<sup>32</sup> The ground state of  $^8\text{B}$  which has a separation energy of 140 keV provides perhaps the best example which can be studied experimentally in more detail. The calculated  $0p_{3/2}$  spectroscopic factor between the  $^8\text{B}$  ( $2^+$ ) and  $^7\text{Be}$  ( $3/2^-$ ) ground states is about one, which means that  $^8\text{B}$  can be viewed as a single loosely bound proton outside of  $^7\text{Be}$  together with two more tightly bound protons. The quadrupole moment of this state has been discussed theoretically.<sup>33</sup> The loose binding of the valence nucleons could reduce the coupling to the core protons and hence reduce the value of the effective charge which is required<sup>32</sup> (i.e., the correction due to the coupling with the  $2\hbar\omega$  giant quadrupole state.) This effect is often neglected.

## 16. Di-proton Decay

The proton-rich analogue of  $^{12}\text{Be}$  is  $^{12}\text{O}$ , which is unbound to two-proton decay. Simple cluster model estimates<sup>34</sup> of the di-proton decay lead to widths which are much too large compared to experiment. More realistic three-body models<sup>35</sup> which take into account the complex shell-model structure would be interesting to explore. The general experimental and theoretical understanding of di-proton decay, which include the cases  $^6\text{B}$ ,  $^{12}\text{O}$ ,  $^{16}\text{Ne}$ , and those in the  $A=39-48$  region,<sup>34</sup> is an open problem.

## 17. Isobaric Analogue States

The relative binding energies (displacement energies) of isobaric analogue states depend on the structure. For those states whose predominant structure is that of a single-particle outside of a core, the Woods-Saxon model calculation, in which the one-nucleon separation energy is fixed to the experimental value, provides a semi-quantitative understanding of the displacement energies.<sup>36</sup> The displacement energies depend on the valence density (mainly the rms radius) and are thus a useful source of information even for excited states. Perhaps the best example of this is the 400 keV downward shift in the excitation energy of the  $1/2^+$  state in  $^{17}\text{F}$  relative to  $^{17}\text{O}$  (this is sometimes called the Thomas-Ehrman shift). It would be interesting to have better information on the analogues of the  $^{11}\text{Be}$  parity doublet. In particular, it has been suggested<sup>37</sup> that the ground state of  $^{11}\text{N}$  is not the relatively narrow state observed in the ( $^3\text{He}, ^6\text{He}$ ) transfer reaction,<sup>38</sup> but is a broad  $1/2^+$  state about 1 MeV lower in energy. There should be many such states which are worth further experimental and theoretical investigation.

In other cases where the structure is more complicated, configuration mixing must be included. However, the many-body treatment of the problem limits most configuration mixing calculations to the harmonic-oscillator basis, and thus they do not account properly for the Thomas-Ehrman shift. Nevertheless the configuration mixing calculations<sup>39</sup> clearly show the dominance of the Coulomb contribution and the



need for a charge-dependent nuclear interaction – a two percent greater attraction in the proton-neutron ( $T=1$ ) interaction compared to the average of the proton-proton and neutron-neutron interactions.

## 18. State-Dependence of the Effective Interactions

As mentioned above, one of the assumptions behind the model-independent effective interactions is that the two-body matrix elements themselves are the same for every energy level and every nucleus, with, at most, a smooth mass dependence. Is this reasonable, especially for states whose rms radius is abnormally large? This is difficult to answer without a better microscopic understanding of the many-body problem. Phenomenologically the same interaction appears to work equally well for bound states, excited states and nuclei near the drip line.<sup>9,24</sup> This may be due to the density dependence of the effective interaction which makes the interaction relatively weaker at higher density in the nuclear interior. Thus the density dependence which will increase the interaction at larger radii (smaller density) will tend to cancel the decrease due to the geometrical dependence. This can be seen in the simple density-dependent delta interaction used by Bertsch and Esbensen.<sup>40</sup> Further investigation of this problem could come from the “dynamical” shell-model approach<sup>41</sup> of Otsuka et al., which combines aspects of the density-dependent Hartree-Fock and configuration-mixing approaches.

## 19. Fermi Beta Decay

Superallowed Fermi beta decay in nuclei is important for a precise test of unitarity in the standard model of weak interactions. The most uncertain aspect (at the level of about 0.3 percent in the decay rate) is the role of isospin mixing in reducing the nuclear overlap matrix elements.<sup>42,43</sup> These isospin mixing corrections are  $Z$ -dependent, and since  $^{14}\text{O}$  has the smallest  $Z$  value of the accurately measured decays, the  $^{14}\text{O}$  decay plays a particularly important role in the extrapolation of the Fermi matrix element to  $Z=0$ . The  $^{10}\text{C}$  Fermi decay<sup>44</sup> may be improved to an interesting level. It will be important to make better use of the connections between displacement energies, asymmetry in mirror Gamow-Teller beta decay, and corrections to the Fermi beta-decay.

## 20. Gamow-Teller Beta Decay

Gamow-Teller (GT) beta decay in light nuclei is important because of the very simple nature of the GT operator and because a complete ( $0\hbar\omega$ ) wave function basis can be used. The large overall quenching of the strength in both the  $0p$ <sup>45</sup> and  $0d1s$  shells<sup>46</sup> is particularly striking and has been understood<sup>47,48</sup> in terms of higher-order configuration and  $\Delta$ -particle nucleon-hole mixing. In most cases only a fraction of the Gamow-Teller strength falls within the beta-decay  $Q$ -value window. Exceptions to this are the decay of  $^6\text{He}$ ,  $^7\text{Be}$ ,  $^{18}\text{Ne}$ ,  $^{18}\text{F}$  and  $^{19}\text{Ne}$ . The beta decay of nuclei near

the drip lines and the subsequent delayed particle emission<sup>49</sup> provide a simple and important test of the nuclear models.

## 21. Gamow-Teller Excitations in $^{16}\text{O}$

GT and M1 excitation of the  $^{16}\text{O}$  ground state are forbidden in the closed-shell  $0\hbar\omega$  model space. Thus the observed strength provides a direct test of the higher-order correlations, which are also responsible for the quenching of the allowed GT discussed above. GT strength has been observed in (p,n)<sup>50</sup> and (p,p')<sup>51</sup> reactions to a few discreet states at 16-18 MeV in the  $^{16}\text{O}$  excitation energy. Calculations in a  $(0+2)\hbar\omega$  model space<sup>50</sup> predict much too little strength in these low-lying states but a considerable strength spread out over many states up to 30 MeV in excitation energy. More recent calculations<sup>4,12</sup> in a  $(0+2+4)\hbar\omega$  model space predict essentially the same. The  $4\hbar\omega$  mixing in the  $^{16}\text{O}$  ground state is small, and the main effect of the  $4\hbar\omega$  is to push down the energy of the  $2\hbar\omega$   $1^+$  states and to mix with them (causing more spreading of the strength). More recent (p,n) experiments<sup>52</sup> do observe considerable GT strength up to 30 MeV in excitation, but the extracted strength somewhat uncertain due to the subtraction of other multipoles.

We have tried unsuccessfully to improve the calculations for the low-lying  $1^+$  states by investigating the use of other cross-shell ( $\Delta\hbar\omega=2\hbar\omega$ ) interactions. Perhaps there is a problem in extracting GT strength from the (p,p') and (p,n) data for these relatively weak transitions, due for example to two-step contributions. This disagreement remains a puzzle.

## 22. M1 Excitations in $^{16}\text{O}$

M1 strength is experimentally known only for the low-lying states,<sup>50,51</sup> and the  $(0+2+4)\hbar\omega$  calculations<sup>9</sup> are able to reproduce this strength relatively well. Comparison of the experimental GT and M1 strength indicates that the transition operator is dominated by spin excitation, however, the calculated strength is dominated more strongly by orbital excitation.

It is interesting to note that the GT and M1 strength obtained in the ZBM ( $0p_{1/2}$ ,  $0d_{5/2}$ ,  $1s_{1/2}$ ) model space<sup>50</sup> is in relatively good agreement with experiment for the low-lying states. [Also, the results obtained in the  $(0d_{3/2}, 0f_{7/2})$  model space<sup>53</sup> for  $^{40}\text{Ca}$  are in reasonable agreement with the experimental strength in the low-lying  $1^+$  states of  $^{40}\text{Ca}$ <sup>54</sup>]. Although there is no obvious reason why these truncated model spaces should be appropriate, perhaps they will provide some clue to the reason for the disagreement in the low-lying GT strength.

## 23. First-Forbidden Beta Decay

Higher-order beta decay is, in general, complicated because of the many operators involved. The operator which gives rise to the first-forbidden  $0^+ \rightarrow 0^-$  beta decay is, however, particularly simple and interesting. One expects a large enhancement in

the axial-charge part of this matrix element due to meson exchange, and, in fact, this should be one of the most dramatic and direct tests of meson exchange. A recent  $(0+2+4)\hbar\omega \rightarrow (1+3)\hbar\omega$  analysis of four beta decays ( $A=11-16$ ) of this type, together with  $\mu^-$  capture on  $^{16}\text{O}$ , gave an enhancement factor of  $1.61 \pm 0.03$  for the axial-charge matrix element.<sup>55</sup> This analysis illustrated the importance of going beyond the simplest  $0\hbar\omega \rightarrow 1\hbar\omega$  treatment of such transitions.

## 24. Parity Nonconservation

Parity nonconservation for states in light nuclei provides a stringent test of the hadronic weak-interaction models, because the wave functions which can be used are more complete than those in heavier nuclei.<sup>56</sup> Several experiments in the  $A=14-21$  nuclei provide values or good upper limits to the PNC observables. Since the PNC OPEP two-body operator is the same as the OPEP operator which gives rise to the enhancement of the axial-charge part of the first-forbidden beta decay discussed above, the PNC observables in  $^{18}\text{F}$  and  $^{19}\text{F}$  can to some extent be calibrated to the analogous first-forbidden beta-decay.<sup>56</sup> The PNC observables in  $^{14}\text{N}$  and  $^{21}\text{Ne}$  cannot be calibrated in this way, and we have recently emphasized the importance of including higher  $\hbar\omega$  excitations in the analysis of these cases.<sup>57</sup>

## 25. Occupation Numbers and $(e,e'p)$

One-nucleon pick-up reactions have been used for many years to extract spectroscopic factors, and they have provided one of the most simple and successful tests of the nuclear shell model. However, uncertainties in the optical model parameters and in the reaction mechanisms lead to an uncertainty in the extracted spectroscopic factors especially for their absolute value. More recently, the  $(e,e'p)$  reaction has been used to extract spectroscopic factors with the hope that the electromagnetic nature of at least part of the reaction will reduce the uncertainties. Such experiments in general have lead to surprisingly small values of the spectroscopic factors. In particular, a recent  $^{16}\text{O}(e,e'p)$  experiment<sup>58</sup> gave spectroscopic factors of about 0.07, 0.11, 2.51 and 1.27 for the  $0s_{1/2}$ ,  $1d$ ,  $0p_{3/2}$  and  $0p_{1/2}$  for the strength summed over 12 final states in  $^{15}\text{N}$  up to 13 MeV. One might expect these to total to 6, but, in fact, only 66 percent of this strength is found. Even though the  $^{16}\text{O}$  ground state is only about 40 percent  $0\hbar\omega$  in the  $(0+2+4)\hbar\omega$  model space, the occupancies are 0.07, 0.67, 3.66 and 1.60, respectively. In addition, the spectroscopic strength to  $^{15}\text{N}$  associated with these occupancies goes almost entirely to the low-lying states. The reason for the poor agreement with experiment is not understood.

## 26. Electron Scattering

This is a important area with a lot of nice experimental data, but I will touch upon only a few aspects. The nuclear rms charge radii are, of course, a basic input into all shell-model calculations. The charge density profiles from longitudinal elastic

(e,e') appear to be rather well described by the nearly closed-shell occupancies<sup>59</sup> in apparent contradiction to what one inferred from (e,e'p). The stretched high-spin states in transverse electron scattering ( $[0d_{5/2} 0p_{3/2}^{-1}] 4^{-1} \hbar\omega$  in this case) are relatively simple, but the addition of  $3\hbar\omega$  and the mesonic exchange currents complicates the interpretation in terms of occupation numbers. Much experimental and theoretical work has been done on the multipoles inbetween.

## 27. Alpha Clustering

The interplay between alpha clustering and the traditional shell model picture is not clear. How orthogonal are these two models? It would, for example, be interesting to investigate the structure of the well-known 7.65 MeV  $0^+$  state in  $^{12}\text{C}$  in terms of the  $(0+2+4)\hbar\omega$  shell model wave functions and its suggested alpha-cluster structure. Alpha transfer and decay are, of course, very relevant, and the microscopic models pioneered by Arima et al. need to be developed further.<sup>60</sup>

## 28. Astrophysics

With the greatly expanding observational knowledge of the universe, it is more important than ever to quantitatively understand the reaction rates for the various nuclear processes which enter into the structure and evolution of the universe. All of the above topics are important. As recent theoretical examples, I pick rather arbitrarily, the effect of the neutron halo on the S factors for neutron capture,<sup>61</sup> the effect of displacement energies on the structure of proton-rich nuclei important for the rp-process,<sup>62</sup> and weak interaction rates in the  $0d_{1s}$  shell.<sup>63,64</sup>

## 29. Acknowledgement

Support for this work was provided from US National Science Foundation grant number PHY-94-03666.

## 30. Dedication

This paper is dedicated to two people: Akito Arima, who I hope will have 30 more productive years in nuclear physics, and my colleague Ernie Warburton, who passed away on May 9, 1994.

## 31. References

1. B. A. Brown and B. H. Wildenthal, *Annu. Rev. Nucl. Part. Sci.* **38**, 29 (1988).
2. J. P. Elliott and T. H. R. Skyrme, *Proc. R. Soc. London Ser A* **232**, 561 (1955); S. Gartenhaus and C. Schwartz, *Phys. Rev.* **108**, 482 (1957).

3. D. H. Gloeckner and R. D. Lawson, *Phys. Lett.* **53B**, 313 (1974).
4. E. K. Warburton, B. A. Brown and D. J. Millener, *Phys. Lett. B* **293**, 7 (1992).
5. T. Hoshino, H. Sagawa and A. Arima, *Nucl. Phys.* **A481**, 458 (1988).
6. L. Jaqua, M. A. Hasan, J. P. Vary and B. R. Barrett, *Phys. Rev.* **C46**, 2333 (1992).
7. B. A. Brown, W. A. Richter and R. E. Julies, *Ann. Phys.* **182**, 191 (1988).
8. D. J. Millener and D. Kurath, *Nucl. Phys.* **A255**, 315 (1975).
9. E. K. Warburton and B. A. Brown, *Phys. Rev.* **C46**, 923 (1992).
10. A. Arima, H. Horiuchi and T. Sebe, *Phys. Lett.* **24B**, 129 (1967).
11. P. J. Ellis and T. Engeland, *Nucl. Phys.* **A144**, 161 (1970); *Nucl. Phys.* **A181**, 368 (1972) and references therein.
12. W. C. Haxton and C. Johnson, *Phys. Rev. Lett.* **65**, 1325 (1990).
13. A. A. Wolters, A. G. M. van Hees and P. W. M. Glaudemans, *Phys. Rev.* **C42**, 2053 (1990); **C45**, 473 (1992).
14. D. J. Millener, A. C. Hayes and D. Strottman, *Phys. Rev.* **C45**, 473 (1992).
15. D. C. Zheng, B. R. Barrett, L. Jaqua, J. P. Vary and R. J. McCarthy, *Phys. Rev.* **C48**, 1083 (1993); L. Jaqua, P. Halse, B. R. Barrett and J. P. Vary, *Nucl. Phys.* **A571**, 242 (1994); D. C. Zheng and B. R. Barrett, *Phys. Rev.* **C49**, 3342 (1994).
16. H. Sagawa, B. A. Brown and H. Esbensen, *Phys. Lett. B* **309**, 1 (1993).
17. I. Talmi and I. Unna, *Phys. Rev. Lett.* **4**, 469 (1960).
18. R. A. Kryger et al., *Phys. Rev.* **C47**, R2439 (1993); B. M. Young et al., *Phys. Rev.* **C49**, 279 (1994).
19. T. Hoshino, H. Sagawa and A. Arima, *Nucl. Phys.* **A506**, 271 (1990).
20. W. R. Gibbs and A. C. Hayes, *Phys. Rev. Lett.* **67**, 1395 (1991); H. Esbensen, D. Kurath and T. S. H. Lee, *Phys. Lett. B* **287**, 289 (1992).
21. E. K. Warburton, J. A. Becker and B. A. Brown, *Phys. Rev.* **C41**, 1147 (1990).
22. N. Fukunishi, T. Otsuka and T. Sebe, *Phys. Lett. B* **296**, 279 (1992).
23. A. Poves and J. Retamosa, *Nucl. Phys.* **A571**, 221 (1994).
24. B. A. Brown, E. K. Warburton and B. H. Wildenthal in *Exotic Nuclear Spectroscopy*, ed. by W. C. McHarris, (Plenum, 1990) p. 295.
25. F. C. Barker, *J. Phys.* **G2**, L45 (1976).
26. I. Tanihata et al., *Phys. Lett.* **160B**, 380 (1985); I. Tanihata, *Nucl. Phys.* **A552**, 275c (1991).
27. G. F. Bertsch, B. A. Brown and H. Sagawa, *Phys. Rev.* **C39**, 1154 (1989).
28. B. A. Brown in the *Proceedings of the Symposium in Honor of Akito Arima - Nuclear Physics in the 1990's*, Santa Fe, New Mexico, May 1-5, 1990 (North Holland, 1991), p. 221c.
29. H. Sagawa, *Phys. Lett. B* **286**, 7 (1992).
30. D. J. Millener, D. E. Alburger, E. K. Warburton and D. H. Wilkinson, *Phys. Rev.* **C26**, 1167 (1982).
31. N. Fukunishi, T. Otsuka and I. Tanihata, *Phys. Rev.* **C48**, 1648 (1993).

32. B. A. Brown, A. Arima and J. B. McGrory, *Nucl. Phys.* **A277**, 77 (1977).
33. H. Nakada and T. Otsuka, *Phys. Rev.* **C49**, 886 (1994); H. Kitagawa and H. Sagawa, *Phys. Lett. B* **299**, 1 (1993).
34. B. A. Brown, *Phys. Rev.* **C43**, R1513 (1991).
35. B. V. Danilin et al., *Proceedings of the Third International Conference on Radioactive Nuclear Beams*, Michigan State University, May 24-27, 1994, p. 235.
36. R. Sherr and G. Bertsch, *Phys. Rev.* **C32**, 1809 (1985).
37. R. Sherr, private communication.
38. W. Benenson et al., *Phys. Rev.* **C1**, 2130 (1974).
39. W. E. Ormand and B. A. Brown, *Nucl. Phys.* **A491**, 1 (1989).
40. G. F. Bertsch and H. Esbensen, *Ann. Phys.* **209**, 327 (1991).
41. T. Otsuka, N. Fukunishi and H. Sagawa, *Phys. Rev. Lett.* **70**, 1385 (1993).
42. W. E. Ormand and B. A. Brown, *Phys. Rev. Lett.* **62**, 866 (1989); errata in *Phys. Rev. Lett.* **63**, 103 (1989).
43. D. H. Wilkinson, *Z. Phys.* **A348**, 129 (1994), and references therein.
44. M. A. Kroupa et al., *Nucl. Inst. and Meth.* **A310**, 649 (1991).
45. W. T. Chou, E. K. Warburton and B. A. Brown, *Phys. Rev.* **C47**, 163, 1993.
46. B. A. Brown and B. H. Wildenthal, *At. Data Nucl. Data Tables* **33**, 347 (1985).
47. B. A. Brown and B. H. Wildenthal, *Nucl. Phys.* **A474**, 290 (1987).
48. A. Arima, K. Shimizu, W. Bentz and H. Hyuga, *Adv. Nucl. Phys.* **18**, 1 (1987); I. S. Towner, *Phys. Rep.* **155**, 264 (1987).
49. B. A. Brown, *Phys. Rev. Lett.* **65**, 2753 (1990).
50. K. A. Snover, E. G. Adelberger, P. G. Ikossi and B. A. Brown, *Phys. Rev.* **C27**, 1837 (1983).
51. C. Djalali, et al., *Phys. Rev.* **C35**, 1201 (1987).
52. K. H. Hicks, et al., *Phys. Rev.* **C43**, 2554 (1991); D. J. Mercer et al., *Phys. Rev.* **C49**, 3104 (1994).
53. B. A. Brown, D. J. Horen, B. Castel and H. Toki, *Phys. Lett.* **127B**, 151 (1983).
54. T. N. Taddeucci, et al., *Phys. Rev.* **C28**, 2511 (1983).
55. E. K. Warburton, I. S. Towner and B. A. Brown, *Phys. Rev.* **C49**, 824 (1994).
56. E. G. Adelberger and W. C. Haxton, *Ann. Rev. Nucl. Part. Sci.* **35**, 501 (1985).
57. M. Horoi, G. Clausnitzer, B. A. Brown and E. K. Warburton, to be published in *Phys. Rev. C*; M. Horoi and B. A. Brown, submitted to publication.
58. M. Lueschner et al., *Phys. Rev.* **C49**, 955 (1994).
59. B. A. Brown, S. E. Massen and P. E. Hodgson, *J. Phys.* **G5**, 1655 (1979).
60. M. Grigorescu, B. A. Brown and O. Dumitrescu, *Phys. Rev.* **C47**, 2666 (1993), and references therein.
61. T. Otsuka et al., *Phys. Rev.* **C49**, R2289 (1994).
62. B. A. Brown et al., *Phys. Rev.* **C48**, 1456 (1993).

63. T. Oda et al., *At. Data and Nucl. Data Tables*, **56**, 231 (1994).
64. T. Kajino et al., *Nucl. Phys. A***480**, 175 (1988).